



Modelling spatiotemporal tendencies of climate types by Markov chain approach : A case study in Sanliurfa province in the south-eastern part of Turkey

ALI DEMIR KESKINER* and MAHMUT CETIN**

**Department of Agricultural Structures and Irrigation, Faculty of Agriculture, Harran University, Sanliurfa, Turkey*

***Department of Agricultural Structures and Irrigation, Faculty of Agriculture, Cukurova University, Adana, Turkey*

(Received 31 July 2021, Accepted 23 December 2022)

*e mail : adkeskiner@harran.edu.tr

सार — जलवायु प्रकार की स्थानिक कालिक प्रवृत्तियों की पहचान से जल प्रबंधकों को पानी की मांग वाले क्षेत्रों पर सूखे के नकारात्मक प्रभावों को कम करने में मदद मिल सकती है। इस अध्ययन का प्राथमिक उद्देश्य एरिक (Erinc's) के शुष्कता सूचकांक (ईडीआई) का उपयोग करके सैलिउर्फा प्रांत में जलवायु-प्रकारों की स्थानिक कालिक प्रवृत्तियों का पता लगाना था। जिसके लिए, दीर्घकालिक (1965-2018) वार्षिक वर्षण और मौसम विज्ञान स्टेशनों की औसत वार्षिक अधिकतम तापमान श्रृंखला प्राप्त की गई और वार्षिक आधार पर ईडीआई श्रृंखला की गणना करने के लिए उपयोग की गई। प्रत्येक स्टेशन की ईडीआई श्रृंखला को तीन अवधियों, गैर-अतिव्यापी और क्रमिक, यानी P1 (1965-1981), P2 (1982-1999) और P3 (2000-2018) में विभाजित किया गया था। बाहरी कारकों का पता लगाकर ईडीआई श्रृंखला से हटा दिया गया; अनुपलब्ध डेटा को समाश्रयण विश्लेषण द्वारा पूरा किया गया। प्रत्येक स्टेशन के लिए तीन अवधियों के लिए जलवायु वर्गों के मार्कोव संक्रमण संभाव्यता मैट्रिक्स (आव्यूह) का अनुमान लगाया गया। प्रत्येक जलवायु वर्ग की तीन अवधियों के लिए प्रारंभिक संभाव्यता सदिश और स्थिर-अवस्था संभाव्यताओं के मानचित्र प्रतिलोम दूरी-भारित तकनीक द्वारा उत्पन्न किए गए। प्रत्येक जलवायु वर्ग के साथ-साथ अवधि के लिए हाइपोमेट्रिक वक्र विकसित किए गए, और घटना संभाव्यताओं (ओपी) का क्षेत्रीय कवरेज निर्धारित किया गया। परिणामों से संकेत प्राप्त हुआ कि जैसे-जैसे समय आगे बढ़ा, गंभीर-शुष्क और शुष्क जलवायु वर्गों की क्षेत्रीय सीमा दक्षिण से उत्तर की ओर लगातार फैलती रही। अर्ध-शुष्क जलवायु प्रकार के क्षेत्रों का शुष्क-जलवायु प्रकार की ओर थोड़ा सा रुझान दिखा। इस क्षेत्र में बड़े बांधों का निर्माण शुष्क क्षेत्रों के विकास के पक्ष में जलवायु परिवर्तन को नहीं रोक सका। आर्द्र जलवायु वर्ग के भविष्य में लुप्त होने की संभावना है। अनुसंधान ने हमें यह निष्कर्ष निकालने के लिए प्रेरित किया कि दक्षिण से उत्तर की ओर शुष्क क्षेत्र का विस्तार जल संसाधनों की पर्याप्तता के संदर्भ में खतरनाक रहा है। यह दृढ़ता से अनुशंसा की जाती है कि क्षेत्र के लिए वन प्रबंधन प्रथाओं के साथ समय-समय पर स्थानिक कालिक जलवायु परिवर्तन अध्ययन आयोजित किए जाने चाहिए।

ABSTRACT. Identification of spatiotemporal tendencies of climate types may help water managers mitigate the negative impacts of droughts on water-demanding sectors. The primary objective of this study was to figure out the spatiotemporal tendencies of climatypes in Sanliurfa province by using Erinc's aridity index (EDI). To that end, long-term (1965-2018) annual precipitation and average annual maximum temperature series of meteorological stations were obtained and utilized to calculate the EDI series on a yearly basis. The EDI series of each station was divided into three periods, non-overlapping and successive, *i.e.*, P1 (1965-1981), P2 (1982-1999) and P3 (2000-2018). Outliers were detected and removed from the EDI series; missing data were completed by regression analysis. The Markov transition probability matrix of the climate classes for the three periods was estimated for each station. Maps of the initial probability vectors and steady-state probabilities for the three periods of each climate class were generated by the inverse distance-weighted technique. Hypsometric curves for each climate class, as well as period, were developed and areal coverage of occurrence probabilities (OP) was determined. Results indicated that, as time progressed, the areal extent of severe-arid and arid climatic classes continued consistently to spread from the south to the north. Areas of semi-arid climate type showed a slight tendency towards the arid-climate type. Construction of large dams in the region could not

prevent the shifts in the climate in favour of developing arid zones. The humid climate class is likely to vanish away in the future. Research led us to conclude that the expansion of the arid zone from south to north has been alarming in terms of the adequacy of water resources. It is strongly recommended that spatiotemporal climate change studies should be periodically conducted in tandem with forest management practices for the region.

Key words – Drought, Spatiotemporal variability, Southeastern Anatolia Project (GAP in Turkish), Probabilistic modeling, Markov chains.

1. Introduction

The weather reflects the day-to-day temperature, precipitation, humidity, etc., of the atmosphere at any given time and location. However, the climate is defined not only by average temperature, precipitation, humidity, etc., over longer periods of decades to centuries but also by the type, frequency, duration and intensity of weather events such as heat waves, cold spells, storms, floods and droughts (USEPA, 2021). With a long-term increase in global average temperatures, Earth's climate system - consisting of the atmosphere, ocean, land surface, ice and snow surfaces (both land and ocean areas) and the biosphere- is affected by anthropogenic interventions and this phenomenon is universally called global warming by various authors and organizations (Houghton, 2002; Speight, 2019). In this context, the term “global warming” is frequently used interchangeably with the term “climate change”, though global warming refers to both anthropologically and naturally produced warming (NASA, 2021a). It has been clear evidence that human influence has been preponderantly dominant in the warming of the atmosphere and the ocean, changes in the global water cycle, reductions in snow-course and ice-pack and a rise in global mean sea levels. Based on the scientific findings, IPCC (2013) had concluded that human influence has been the dominant cause of observed warming since the mid-20th century. As addressed by many researchers, anthropogenic activities have been among the most important factors causing an increase in the temperature of the Earth in the last 50 years (NASA, 2021b). As a result, the atmosphere and the ocean have warmed, the amounts of snow- and ice-packs have remarkably diminished and the sea level has conspicuously risen lately (IPCC, 2014). In this context, increases in average global temperatures have been expected to be within the range of 3°C to 5°C by 2100 (WMO, 2019). Because temperature is an indication of heat energy and when some energy is added to any system, the changes are likely to be seen visually in the system. For example, it has been reported that the frequency of droughts and floods has revealed remarkable spatiotemporal changes in different climatic regions over the world due to global warming. Albeit the causes of abrupt climate changes have not been established, its impacts on local marine systems, global hydrological cycle, soil-water balance and terrestrial ecosystems across

continents have shown that climate change-induced events such as sea level rises, frequency and severity of floods and droughts, shortage of ground water and surface water bodies, etc. have been triggered (NRC, 2002; Kumar *et al.*, 2011) for a few decades. The prevalence and dominance of droughts as stated by Keskiner *et al.* (2020) are relevant to climate change as well as to climate variability. On the other hand, some regions in the world are more prone to severe droughts than other regions. In this context, as clearly addressed by Li *et al.* (2017), it has been globally accepted that Mediterranean countries, including Turkey, have been experiencing more frequent as well as severe drought events lately. Though Turkey is located between the mid-latitude temperate climate zone and subtropical climate zone, it is under the influence of a Mediterranean-type macro-climate. In turn, seven different climate regimes are dominant in Turkey. Nevertheless, it has already been considered among the risk group countries in terms of the possible effects of climate change and global warming. Iyigun *et al.* (2013) and Turan (2018), among others, pointed out that Turkey would be adversely affected by climate change and global warming in the future. This situation is a major negative effect of climate change on water availability for food security and production, rural development and increased incidence of crop and livestock pests and diseases (Panwar *et al.*, 2020; UNDP, 2021). Moreover, the decrease in the amount of precipitation aggravates the severity of droughts as well as the state of aridity and the expansion of arid zones in a region. Soon, arid and semi-arid regions may face great calamities induced by climate change. For example, according to the findings obtained from simulations of global climate models, an increase in both frequency and intensity of the heat waves is to be expected particularly in the Eastern and Southeastern Anatolia Regions of Turkey during the 2015-2100 projection period (FFDIA, 2017). Large-scale integrated regional development projects such as Southeastern Anatolia Project (GAP in Turkish) in Turkey (Cetin, 2020) may be a remedy both in coping with droughts and in eliminating the arid-zone encroachment on semiarid zones.

The GAP is a world-renowned integrated development project, aiming at the socio-economic development of the region predominantly through irrigation and energy investments in the Tigris-Euphrates

twin river basin located in the Southeastern Anatolia Region of Turkey (Loucks and van Beek, 2005; Cetin, 2020). Therefore, the GAP, which is one of the largest of its kind in the world, consists of building 22 dams, 19 hydroelectric power plants and components of irrigation projects in the Southeastern Anatolia Region (Komuscu *et al.*, 1998; Cetin, 2020). Since the GAP area, highly prone to aridity, is located in a semi-arid region in Turkey, agricultural production is limited by the lack of rainfall during the growing period of the commonly grown crops. Thus, irrigation is inevitable in the area to develop a highly productive agricultural system. Therefore, after the completion of the GAP, 1.78 Mha area (21% of the targeted irrigation potential of Turkey) will have been equipped with irrigation facilities, 1.19 Mha of which is in the Euphrates sub-basin and 0.59 Mha in the Tigris sub-basin. Harran Plain (151 419 ha irrigable area), constituting a major irrigation area of the GAP, is completely located in Sanliurfa province. The semi-arid climate type (Caglak *et al.*, 2016; Inceyol and Cay, 2017) is preponderant over the environs of Sanliurfa province. Hence, the region has experienced severe drought events of different durations, causing grave irrigation water-sharing problems in the Harran Plain irrigation scheme, which is under the influence of arid and severe arid climate types prevalent in the Syrian territory.

Therefore, monitoring drought propagation and the spatiotemporal tendencies of climate types over time is of great importance in the environs of Sanliurfa. In order to detect the change and/or spatial extent of drought, it is essential to use drought indices as well as indicators. In this context, a myriad of methods or indices has been developed to characterize the state of drought or climate class of a region. Although the global climate models and climate classification methods have undergone continuous developments, there remains considerable uncertainty about the local and regional environmental consequences of the changing climate (Feddema, 2005; Savo *et al.*, 2016; Habibi *et al.*, 2018; Singh *et al.*, 2018). Köppen climate classification, Aydeniz method, Erinc's drought index, percentage of normal index, standardized precipitation index, Palmer drought severity index, Thornthwaite and De Marton methods, just to name but a few, are among the frequently used ones in regional climate classification studies in Turkey (Keskiner *et al.*, 2019; TSMS, 2021). Besides, the occurrence probabilities of droughts, drought periods or each climate class may be predicted by the Markov chain analysis. Thus, significant differences between the two climate regions may be determined by modelling the spatiotemporal tendencies of climate types (Mieruch *et al.*, 2010; Fidan, 2011; Reis and Dotal, 2016). To make reasonable inferences about regional changes in climate classes observed in sequential time periods (*e.g.*, in months, years or decades), it is to



Fig. 1. Location of the study area in Turkey and spatial distribution of meteorological stations

determine the spatiotemporal trends of climate classes in arid and semi-arid regions in particular (Han *et al.*, 2015).

The staple objectives of this study are twofold: (a) to investigate the spatial extent of climate classes/types by Erinc's drought index in sequential periods at an annual times-scale (Period 1: 1965-1981, Period 2: 1982-1999, Period 3: 2000-2018) and (b) to figure out the likely impacts of large-scale water resources development projects materialized in a semi-arid to a desert-type environment on developing climate types in three sequential periods.

2. Materials and methods

2.1. Study area and data

This research was carried out within the borders of Sanliurfa province (Fig. 1), covering 19 242 km² area (37°51' 19.3" - 40°13' 46.6" E longitudes and 36°40' 08.1" - 38°01' 24.8" N latitudes), located in the Southeastern Anatolia Project (GAP in Turkish) area (GDM, 2021), in southeastern Turkey. The long-term annual total precipitation and annual maximum temperature observations of Sanliurfa, Birecik, Akcakale, Ceylanpinari and Siverek meteorological stations from 1965 to 2018 and of Bozova meteorological station from 2000 to 2018 were utilized to generate Erinc's drought

TABLE 1

Erinc's classification of climate types and coding for Markov chain analysis

Climate Types	Index Value (I_m)	Vegetation Cover	Climate Classification Code (Ci)
Severe-arid	<8	Desert	C1
Arid	8-15	Desertification	C2
Semi-arid	15-23	Arid	C3
Sub-humid	23-40	Forest	C4
Humid	40-55	Moist forest	C5
Very humid	>55	Very moist forest	C6

index series. Geographical locations of the meteorological stations -belonging to the Turkish State Meteorological Service (Fig. 1) - were related to the World Geodetic Reference System, *i.e.*, WGS84, by using Universal Transverse Mercator (UTM) projection to generate probability maps of climate types by the periods considered.

Features of continental climate predominate in Sanliurfa province and its environs. The elevation for downtown, *viz.*, Sanliurfa, is about 518 m above the mean sea level (AMSL). Caglak *et al.* (2016) pointed out that total annual precipitation in Akcakale and Ceylanpinari districts, located in the southernmost zone of the study area, varies between 277 and 310 mm, whereas it reaches up to 900 mm in the north, *i.e.*, around Siverek district of high hills and rolling topography. The average annual temperature varies from 11 °C to 19 °C and temperatures are high in the south of Sanliurfa province, *i.e.*, along the Syrian border, due to the lowest elevation in the study area and topography consisting of flat and slightly sloping. Consequently, the hot air masses, particularly in the summer period, that develop under the influence of the Basra Low-Pressure Center, aggravate the formation of droughts from south to north in Sanliurfa province and its environs located in the GAP area.

2.2. Erinc's Drought/Aridity Index (I_m)

Erinc's Aridity Index (I_m or *EDI*) developed by Erinc in 1965, also known as the precipitation efficiency index, is a drought indicator to describe the drought problem in arid/humid areas (Li *et al.*, 2017; Aydın *et al.*, 2019). I_m is calculated as follows:

$$I_m = \frac{P}{\bar{T}_{max}} \tag{1}$$

Where I_m is the Erinc's aridity/drought index; P and \bar{T}_{max} are annual total precipitation (mm) and average maximum temperature (°C) observed in a given year,

respectively. Mean maximum temperatures less than 0 °C are not considered in I_m calculations.

In this research, Erinc drought index values computed for each year were used to characterize spatiotemporal changes in climate types in a semi-arid region. I_m time series of each station was divided into three non-overlapping and successive parts or periods of nearly two-decade, *i.e.*, period 1 (P1: 1965-1981), period 2 (P2: 1982-1999), period 3 (P3: 2000-2018). I_m time series data of each station were coded, if any, C1 (severe-arid), C2 (arid), C3 (semi-arid), C4 (sub-humid), C5 (humid) and C6 (very-humid) by using I_m value category given in Table 1.

2.3. Detection of outliers

The extreme values that show statistically significant differences from other values in the data set are called outliers. Markov-chain models invariably suffer from challenges arising from the existence of outliers in datasets. In this study, outliers in the I_m series were determined by the T_n statistics given in Grubbs (1969). Suppose that the observation series consists of n observations and it is denoted in order of increasing magnitude by $X_1 \leq X_2 \leq X_3 \leq \dots, < X_n$. Let X_n be the doubtful value (outlier), *i.e.*, the maximum or the minimum value in the data series. The test criterion T_n , recommended by Grubbs (1969) for a single outlier, is calculated as follows:

$$T_n = \frac{|X_n - \bar{X}|}{S} \tag{2}$$

where X_n is the suspected or doubtful observation; \bar{x} is the arithmetic mean of all n values and S is the standard deviation of sample data. If the calculated value of T_n is greater than the tabulated value, X_n is the outlier (Grubbs, 1969; Kesici and Kocabaş, 1998). In this research, outliers in the Erinc's Aridity Index (I_m) series of each station for the three distinct periods were detected ($\alpha = 5\%$).

2.4. Regression analysis

After outlier detection in the I_m time series data, if any, they are excluded from the series and this value was considered as missing data. To complete the missing data in I_m series, firstly, correlations between the station with missing data and nearby ones with the highest Pearson correlation coefficient (r) have been calculated and evaluated. In selecting the best regression model, the determination coefficients (R^2), standard errors and ANOVA results of the models were considered by following the method specified in Landau and Everitt (2004) and Ryan *et al.* (2012). Missing I_m data were estimated by using the linear, quadratic and cubic polynomial regression models given in Equation 3. After the reconstruction of outliers in I_m data using regression models, Climate Classification Codes given in Table 1 were assigned to the completed I_m time series data and Markov chain analysis was done to establish the transition probability matrix of climate types for the three periods of each station.

$$\left. \begin{aligned} P &= b_0 + b_1 X + e \\ P &= b_0 + b_1 X + b_2 X^2 + e \\ P &= b_0 + b_1 X + b_2 X^2 + b_3 X^3 + e \end{aligned} \right\} \quad (3)$$

where P is the dependent variable; X is the independent variable; b_i are the regression coefficients; e is the error term.

2.5. Markov chains modeling

The literature review has revealed that Markov models have been extensively used in climatology and hydrology (Shevnina and Silaev, 2019). A Markov chain is specified as follows: Let $S = \{S_1, S_2, S_3, \dots, S_n\}$ be a set of states. The Markov process starts in a particular state and moves successively from one state to another (Grinstead and Snell, 2012). The movement of the system from one state (S_i) to another (S_j) is called a step and the changes in the state of the system, *i.e.*, $i \rightarrow j$, are called transitions. The probability distribution of state transitions is most conveniently represented in a square array that is called transition probabilities (P_{ij}) or transition probability matrix which is independent of the time (t) (Karamouz *et al.*, 2003; Taha, 2007); Let $X(t)$ denote the state of the system at time t . Then, the transition probabilities P_{ij} might be defined as follows:

$$P_{ij} = P\{X(t + 1) = S_j | X(t) = S_i\} \quad (4)$$

Transition probabilities are commonly illustrated in a transition probability matrix P of $S \times S$ dimension as:

$$P = \begin{bmatrix} P_{11} & P_{12} & \dots & P_{1S} \\ P_{21} & P_{22} & \dots & P_{2S} \\ \cdot & \cdot & \cdot & \cdot \\ \cdot & \cdot & \cdot & \cdot \\ P_{S1} & P_{S2} & \dots & P_{SS} \end{bmatrix} \quad \text{by agreeing with } 0 \leq P_{ij} \leq 1 \text{ and}$$

$$\sum_{j=1}^n P_{ij} = 1 \text{ for all } i, j \in S.$$

Let P be the transition matrix of a Markov chain and let u be the initial probability vector of the system. Then the probability that the chain is in state S_i after n -step is the i^{th} entry in the vector:

$$u^{(n)} = uP^n, \quad n = 1, 2, 3, \dots \quad (5)$$

In this research, Coded Climate Classification (CC) data series, consisted of C1 (severe-arid), C2 (arid), C3 (semi-arid), C4 (sub-humid), C5 (humid) and C6 (very-humid) coders, of each station for the periods considered was used in order to establish transition probability matrix P of $S \times S$ dimension; then, long-term probability vector of the system, *i.e.*, steady-state probability vector, was obtained for the climate types in the third period. To that end, the marginal (fixed) probability vector-calculated from the transition frequency matrix- was used as the initial probability vector (u) in Equation 5.

2.6. Inverse Distance Weighted Interpolation (IDWI) technique

The Inverse Distance Weighted Interpolation (IDWI) technique is one of the most commonly used spatial estimation methods that render estimations of cell values by averaging the values of sample data points in the neighbourhood of each processing cell. By assigning more weights to the observed data close to the point to be estimated, the effect of the nearby observations/stations on the prediction is increased (Cetin and Diker, 2003; ESRI, 2021). In order to generate probability maps for the climate types, *i.e.*, climate-class, the IDWI technique was employed in estimating occurrence probabilities of each climate-class at the grid points (Equation 6). To this end, a grid system having a cell size of 100 m by 100 m was established over the study area and then, the initial probability vectors of P1Ci, P2Ci, P3Ci and the stationary occurrence probabilities of S_P3Ci maps (P_i , C_i and S stand for the period, climate-class and steady-state probability, *i.e.*, $u^{(n)}$ in Equation 5, respectively) for each climate type based on Erinc's Aridity Index (I_m) were generated for the three successive periods in Geographical Information Systems (GIS).

TABLE 2
Descriptive statistics of datasets for the complete observation period of 1965-2018

Statistics	Mean	Median	Stdev.	Skewness	Kurtosis	Minimum	Maximum	N	
Siverek	<i>P</i>	563.9	543.0	146.7	0.47	-0.35	304.0	893.0	54
	<i>Tmax</i>	22.2	22.2	0.9	-0.20	0.12	19.9	24.4	54
	<i>Im</i>	25.6	24.3	7.1	0.61	0.11	13.4	43.8	54
Birecik	<i>P</i>	362.4	347.0	103.6	0.53	-0.28	187.0	614.0	54
	<i>Tmax</i>	25.5	25.6	1.1	-2.23	9.32	20.2	27.1	54
	<i>Im</i>	14.3	13.8	4.3	0.53	-0.20	7.0	25.2	54
Bozova	<i>P</i>	391.9	342.9	106.7	0.71	-0.51	251.1	621.8	19
	<i>Tmax</i>	23.9	24.0	0.7	-0.71	0.75	22.2	25.2	19
	<i>Im</i>	16.5	14.8	4.6	0.62	-0.70	10.4	25.2	19
Sanliurfa	<i>P</i>	448.9	441.5	146.6	0.86	0.61	196.0	855.0	54
	<i>Tmax</i>	24.4	24.6	0.9	-0.22	-0.09	22.0	26.3	54
	<i>Im</i>	18.5	18.2	6.4	0.91	0.76	7.5	35.8	54
Akcakale	<i>P</i>	284.1	266.0	102.2	1.24	2.26	117.0	633.0	54
	<i>Tmax</i>	25.6	25.7	0.8	-0.51	0.32	23.5	27.4	54
	<i>Im</i>	11.2	10.6	4.2	1.21	2.02	4.4	24.8	54
Ceylanpinari	<i>P</i>	298.3	284.5	104.7	0.52	-0.13	109.0	546.0	54
	<i>Tmax</i>	26.3	26.3	0.9	-0.13	-0.04	24.1	27.9	54
	<i>Im</i>	11.4	11.1	4.2	0.56	-0.07	4.1	21.5	54

$$\left. \begin{aligned}
 d_{i0} &= \sqrt{(x_0 - x_i)^2 + (y_0 - y_i)^2} \\
 w_i &= \frac{d_{i0}^{-p}}{\sum_{i=1}^n d_{i0}^{-p}}, \sum_{i=1}^n w_i = 1, \hat{g} = \sum_{i=1}^n w_i g_i
 \end{aligned} \right\} (6)$$

where *n* is the total number of data points used in estimation ($1 \leq n \leq 6$); *d*_{*i0*} is the Euclidean distance (in meters, *m*) between the observed and the estimated point; (*x*₀, *y*₀) is the coordinate for the centroid of the grid (*UTM*, *m*); (*x*_{*i*}, *y*_{*i*}) is the coordinate of the meteorological observation station, *i.e.*, data point, (*UTM*, *m*); *w*_{*i*} are the weights to be assigned for observed points; *p* is a positive real number, called the power parameter (*p* = 2) of IDWI; \hat{g} is the estimated value at the unknown point or in a grid-cell; *g*_{*i*} show the observed values.

2.7. *Developing hypsometric curves : Areal percentage vs. occurrence probabilities of climate types*

In catchment hydrology, a hypsometric curve is essentially a graph that shows the proportion of area that exists at various elevations by plotting relative area against relative height. One approach to analyzing hypsometry is to produce a histogram of the frequency of different elevation bins (Vivoni *et al.*, 2008; Ajaykumar and Gopinath, 2018). In this research, the hypsometric

curves for the long-term occurrence probabilities of climate types or climate-classes were developed for each of the predefined successive periods in order to figure out the spatiotemporal behaviour of climate types. This curve might be a good indicator to define the areal extent of probability of a given climate-class, for example, arid or severe-arid climate-class, by the periods considered.

3. **Results and discussion**

3.1. *Exploratory data analysis results and runs of I_m by years*

Descriptive statistics of the data sets consisting of the long-term (1965-2018) annual total precipitation, annual average maximum temperature and *I_m* series were given in Table 2. Spatial variability of average precipitation and maximum temperature reveals that precipitation has a remarkable decreasing tendency from north to south, while the maximum temperatures increase. Spatial variability behaviour in precipitation and temperature implies that the southern part of the study area is prone to severe drought episodes as addressed by Li *et al.* (2017) and Keskiner *et al.* (2019). In this context, it is noted that the highest average precipitation (563.9 mm) is observed in Siverek of the highest altitude and latitude, located in the utmost north of the study area. However, the average precipitation is the lowest in Akcakale (284.1 mm) located

TABLE 3

Descriptive statistics of EDI series in the three successive periods

Statistics	Mean	Median	Stdev.	Skewness	Kurtosis	Minimum	Maximum	N
Period 1: 1965-1981								
Siverek	26.1	24.2	8.7	0.83	0.32	13.4	43.8	17
Birecik	16.0	16.4	4.4	0.41	-0.44	9.4	25.2	17
Sanliurfa	20.5	19.5	7.5	0.57	-0.05	9.0	35.8	17
Akcakale	12.8	12.2	4.8	0.64	1.31	4.5	24.8	17
Ceylanpınarı	13.8	12.4	4.6	0.02	-0.19	4.6	21.6	17
Period 2: 1982-1999								
Siverek	26.2	25.2	7.1	0.27	-0.50	15.10	39.40	18
Birecik	13.7	13.1	3.9	1.38	2.14	8.90	23.90	18
Sanliurfa	18.7	18.2	6.4	1.18	1.79	10.70	35.20	18
Akcakale	10.7	10.2	3.3	1.06	0.56	6.70	18.60	18
Ceylanpınarı	11.5	10.5	3.9	0.77	-0.15	6.40	19.40	18
Period 3: 2000-2018								
Siverek	24.5	23.1	5.7	0.12	-1.35	15.2	32.9	19
Birecik	13.4	13.8	4.3	0.09	-1.14	7.0	21.2	19
Bozova	16.5	14.8	4.6	0.62	-0.70	10.4	25.2	19
Sanliurfa	16.5	15.5	5.0	0.59	0.36	7.5	28.1	19
Akcakale	10.1	9.8	4.1	2.04	6.23	4.4	23.7	19
Ceylanpınarı	9.3	8.8	3.0	0.03	-0.55	4.1	14.9	19

at the utmost south of the study area where arid and severe arid climatic zone characteristics are more dominant compared to the other stations. On the other hand, descriptive statistics indicate clearly that neither series are symmetrical. This distributional behaviour indicates that mean values are not representative statistics but median values. Therefore, according to Towler *et al.* (2010), skewness and kurtosis coefficients in Table 2 are compatible with the other descriptive statistics.

Long-term (1965-2018) annual total precipitation and mean annual maximum temperature series were divided into three non-overlapping but consecutive periods and Erinc's Drought Index (I_m) on a yearly basis was computed for these periods. Descriptive statistics of the I_m series for the three successive periods were presented in Table 3. It is obvious from Table 3 that, irrespective of periods, the I_m series is characterized by a right-skewed distribution. Thereby, the practical implications of using the mean of I_m series for the periods will be misleading (Stedinger, 2017). The use of median values are of great importance in such cases. Surprisingly,

medians and means of I_m series of stations, apart from Siverek station, tend to decrease from period 1 (P1) to period 3 (P3), indicating that the dominant climate type has been shifting from semi-arid to arid in the majority of the study area by decades. The spread of variability, *i.e.*, standard deviation, generally tends to decrease from the first period to the third period showing a sign of stabilization in climate types. This stabilization slants in favor of arid-type climate in the region where semi-arid climate type used to be dominant (Keskiner *et al.*, 2019) in the past.

I_m values of Akcakale, Sanliurfa and Siverek provinces were plotted (Fig. 2) to depict visually the runs of Erinc's Drought Index (I_m) by years consisting of three consecutive periods. As seen from Fig. 1, Siverek station is far from the Syrian border (>120 km) and it is under the influence of Atatürk Dam. Unexpectedly, the dominant sub-humid climate type in P1 and P2, on average, shifted to semi-arid climate type in P3. Furthermore, the linear decreasing trend of I_m values in Siverek station is an indication of encroachment of the semi-arid zone towards

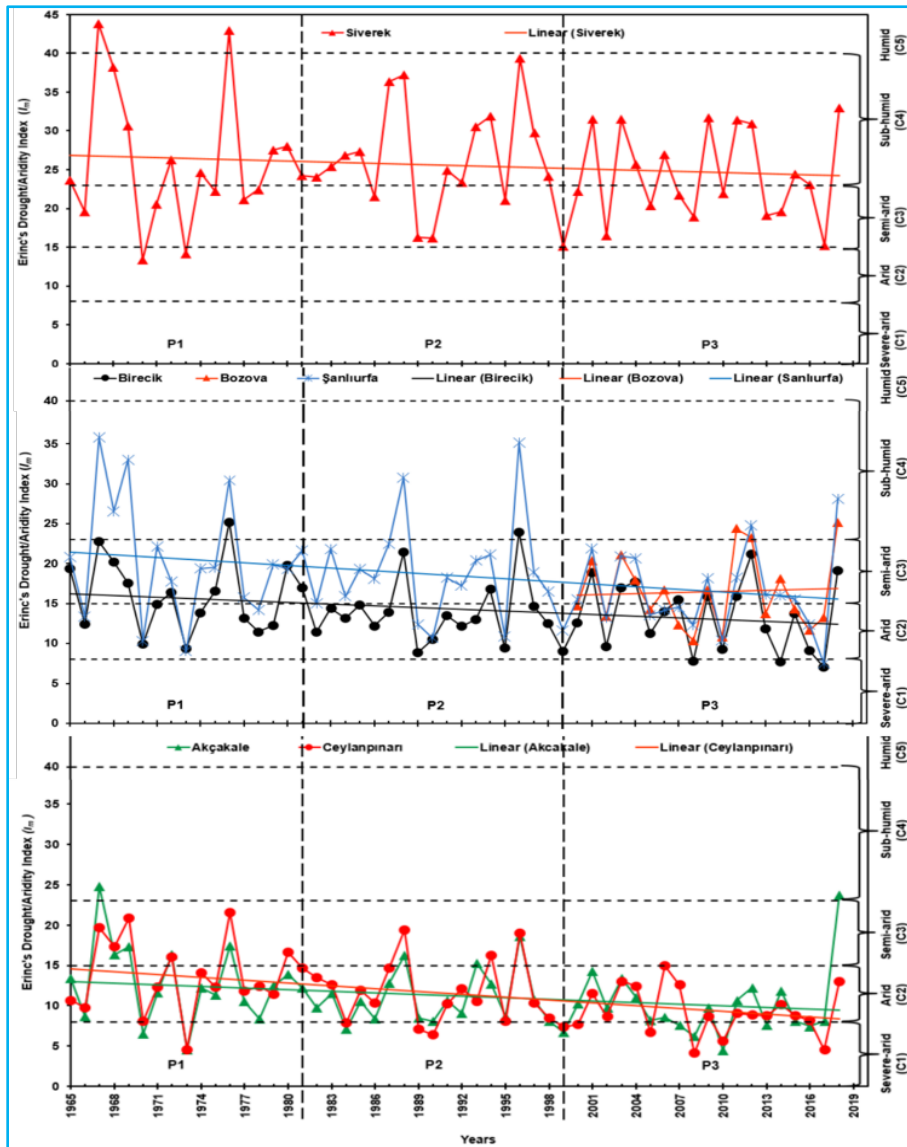


Fig. 2. Temporal trends in I_m of stations located in the utmost south (Akcakale and Ceylanpinari), in central part (Sanliurfa, Birecik and Bozova) and in the utmost north (Siverek) of the study area. P1, P2 and P3 stand for the three periods considered, solid lines are linear trend lines for each station

the north in the study area. It is understood that the climate classes represented by the stations in three different periods tend to be arid and this behavior continues from north to south. It is important to re-emphasize that several large dams were constructed in the study area between 1981 and 1999, *i.e.*, in P2. Tonkaz and Cetin (2007) and Tonkaz *et al.* (2007) pointed out that large dams constructed in the GAP area have affected the climate of the region by increasing water vapor pressure and relative humidity, among others, over the area. As seen from Fig. 2, the decreasing trend in I_m series was curbed, to some degree, in P2; then, the inhibitor impact of water resources development projects on the dominant

climate type, *i.e.*, mostly semi-arid and rarely sub-humid, ended during P3. As a natural consequence of this, the arid climate type in Birecik, Sanliurfa and Bozova stations and severe-arid climate type in Akcakale and Ceylanpinari stations have appeared more frequently lately over the study area, indicating more severe climatic conditions in favor of severe aridity. It may be concluded from exploratory data analysis results that I_m series in the study area has been subject to spatiotemporal variability and characterized by a skewed distribution indicating that mean values are not representative statistics and there exists a gradual shift in climate types from semi-arid to arid and severe-arid climate types.

TABLE 4

Defined outliers in the dataset (X_n stands for the outliers in the series)

Stations	Years and the corresponding period	Year	n	\bar{x}	S	Suspected value (X_n)	T_n	$T_{n(0.05)}$
Akcakale	1965-1981 (P1)	1967	17	12.8	4.8	24.8	2.49	2.47
Sanliurfa	1982-1999 (P2)	1996	18	18.7	6.4	35.2	2.57	2.50
Birecik	1982-1999 (P2)	1996	18	13.7	3.9	23.9	2.61	2.50
Akcakale	2000-2018 (P3)	2018	19	10.1	4.1	23.7	3.30	2.53

TABLE 5

Reconstruction of I_m using linear regression models

	Stations	Akcakale	Sanliurfa	Birecik	Akcakale
Observed outliers as a dependent variable	Altitude (m)	360	550	347	360
	Latitude (m)	4064656	4112732	4096909	4064656
	Period	1	2	2	3
	Year	1967	1996	1996	2018
	Actual I_m	24.8	35.2	23.9	23.7
	Actual CC	C4	C4	C4	C4
	Stations	Ceylanpinari	Akcakale	Sanliurfa	Ceylanpinari
Stations used as the independent variable	Altitude (m)	360	360	550	360
	Latitude (m)	4077686	4064656	4112732	4077686
Correlated stations	r (%)	81	86	85	81
Statistics for regressions	R ² (%)	66	74	72	66
	S	1.9	2.8	2.1	1.9
Results	Estimated I_m	16.1	29.7	21.3	11.8
	Assigned CC	C3	C4	C3	C2

3.2. Outlier detection results

A likely outlier in a data set may distort Markov chain analysis and stability of the transition probability matrix (Grinstead and Snell, 2012). In this context, the most extreme values in I_m series were checked for the periods. The outliers, i.e., suspicious data in Erinc’s aridity/drought index (I_m) series were detected and given in Table 4. As seen from Table 4, the highest I_m values of Akcakale, Sanliurfa and Birecik stations were determined as outliers. More surprisingly, Akcakale station, which has been under severe arid conditions, had outliers in P1 and P3. No conclusion could be reached as to the cause of the outliers.

3.3. Regression analysis results

After detecting outliers, they have been removed from the I_m series to ensure data consistency. Then, to fill

in the gap in the I_m series, Pearson’s correlation coefficient (r) matrix between station pairs was established (Table 5). Based on Pearson's correlation coefficient matrix, linear, quadratic and cubic mathematical models (Equation 3) were utilized to estimate missing data. In this regard, the highest R^2 and the smallest standard error of the estimation were adopted as the model selection criteria. Although the higher models were tried, it was concluded that first-order models as shown in Table 5, i.e., linear ones, were the most suitable ones for completing the missing I_m values at the stations given in Table 4.

The latitudes of Akcakale and Ceylanpinari stations are very close to each other and these stations are at the same altitude (360 m). As seen in Table 5, the linear regression model ($R^2 = 66\%$) established between these two stations has the smallest standard error of the estimation statistics ($S = 1.9$) compared to the other stations. Similarly, regression models for other stations

TABLE 6

The marginal (fixed) probability vectors for the periods (P1Ci, P2Ci, P3Ci) and steady-state n-step transitional probability vector for the period P3 (S_P3Ci)

Periods	Climate Classes	Siverek	Birecik	Bozova	Sanliurfa	Akcakale	Ceylanpinari
P1: 1965-1981	C1	0.0	0.0	N/A*	0.0	11.8	5.9
	C2	11.8	47.1	N/A	23.5	58.8	58.8
	C3	29.4	47.1	N/A	52.9	29.4	35.3
	C4	47.1	5.9	N/A	23.5	0.0	0.0
P2: 1982-1999	C1	0.0	0.0	N/A	0.0	11.1	22.2
	C2	0.0	83.3	N/A	22.2	72.2	61.1
	C3	27.8	16.7	N/A	66.7	16.7	16.7
	C4	72.2	0.0	N/A	11.1	0.0	0.0
P3: 2000-2018	C1	0.0	15.8	0.0	5.3	26.3	26.3
	C2	0.0	42.1	52.6	36.8	73.7	73.7
	C3	47.4	42.1	31.6	47.4	0.0	0.0
	C4	52.6	0.0	15.8	10.5	0.0	0.0
Steady-state n- step transitional probability vector for P3	C1	0.0	16.3	0.0	5.3	27.8	23.5
	C2	0.0	40.3	50.0	36.8	72.2	76.5
	C3	46.2	43.4	30.0	47.4	0.0	0.0
	C4	53.8	0.0	20.0	10.5	0.0	0.0

* Marginal probabilities were not calculated due to insufficient data in the period. C1: Severe-arid, C2: Arid, C3: Semi-arid, C4: Sub-humid

were obtained and missing data were completed as seen in Table 5. It is important to point out that outliers had significant effects on the assigned climate types/codes, indicating the necessity of removing outliers from the data. For example, Akcakale station is located at the Syrian border and the arid (C2) to severe-arid (C1) climate types are preponderant thereabouts. However, as seen in Table 5, if the outlier is neglected, the climate type in the station is assigned as C4 (sub-humid climate type), seeming unrealistic. Substitution of the estimated outlier into the I_m series resulted in a C2 (arid) climate type that makes sense. This kind of interpretation is tolerably compatible with the visible trend behavior in the Fig. 2. Consequently, in modelling spatiotemporal tendencies of climate types through using the first-order Markov chain approach, outliers in the datasets need to be considered in order to deal with the uncertainties in the results. In this regard, results led us to conclude that regression analysis may be considered a simple but effective remedy for completing missing data in drought monitoring, assessment as well as modelling.

3.4. Markov chains analysis results

After having excluded the outliers from the data sets, then the data estimated by the regression technique were

substituted for the missing data for Markov modelling. Later on, Markov transition probability matrix of the climate classes for each period was formed by considering five states, *i.e.*, climate classification codes C_i given in Table 1. As a reminder, State 1 (S_1) was considered as C1, State 2 as C2, etc. Except for Siverek station, not surprisingly, humid (C_5) climate class/type has not been observed in the study area since 1965. Put another way, C_5 was observed only two times in Siverek station in P1 (1965-1981) and has not been observed since then, indicating that climate types have been changing slowly but surely, in favour of arid ones, over a long period of time. In turn, only 4 climate-states were considered in the construction of transition probability matrices. Based on the Markov chain analysis results, marginal (fixed) probability vectors for the periods (P1Ci, P2Ci, P3Ci; $i = 1, 2, 3, 4$) and steady-state n -step transitional probability vectors, *i.e.*, stationary transition probabilities, for the period P3 (S_P3Ci) were given in Table 6.

According to the marginal probability vectors, severe-arid climate type was not observed in Siverek, Birecik and Sanliurfa stations in P1 and P2 periods. However, the occurrence probabilities of severe-arid climate types at Akcakale and Ceylanpinari stations that were located by the Syrian border were 11.1% and 22.2%

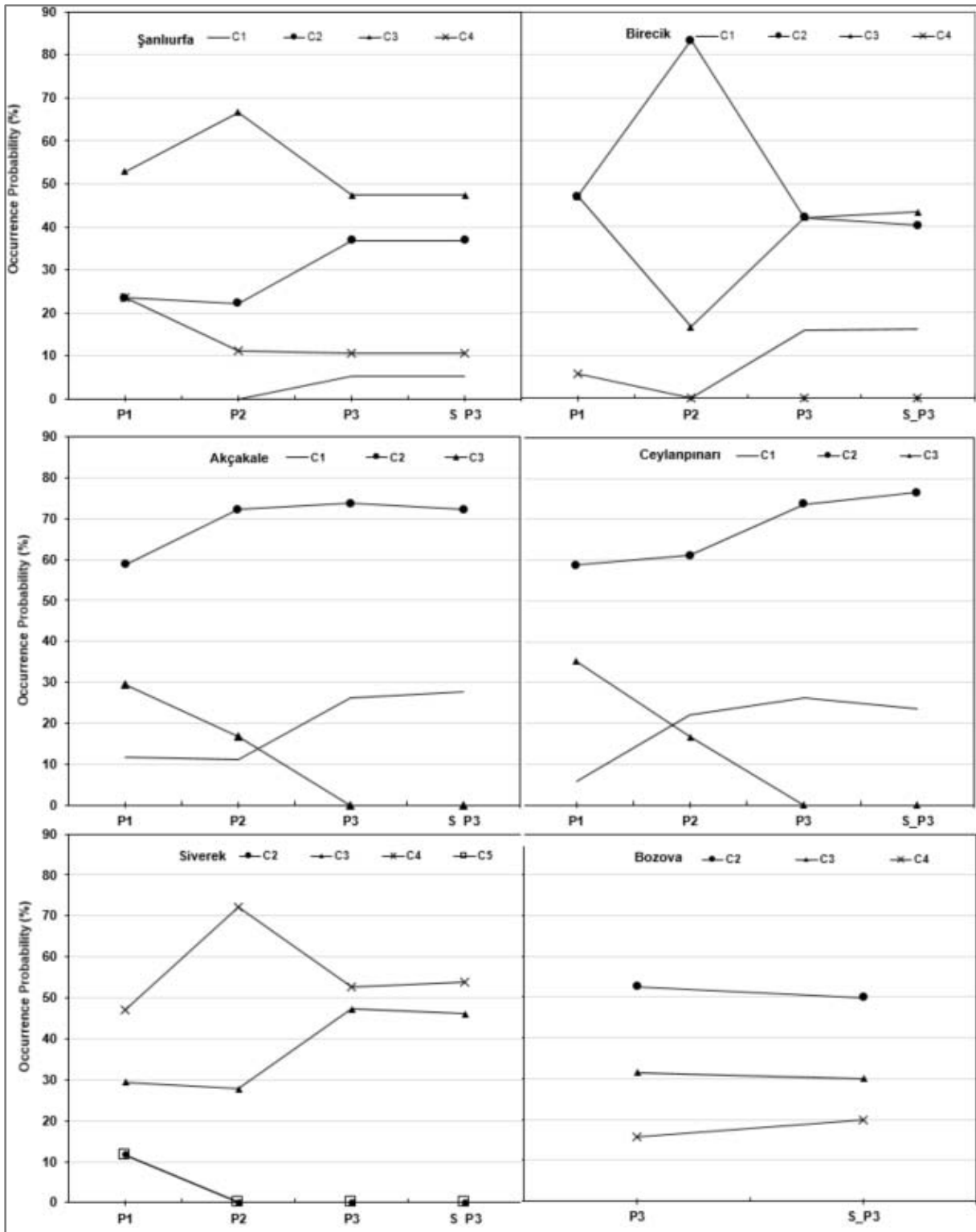


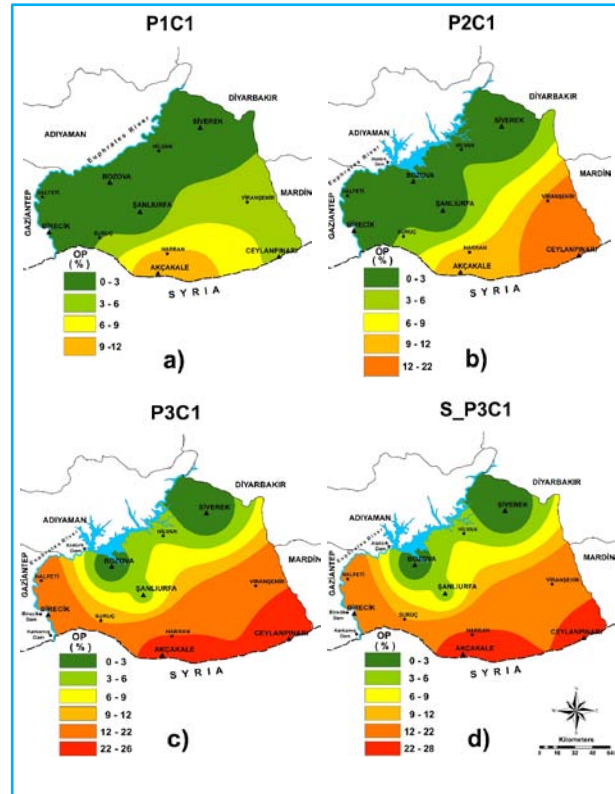
Fig. 3. Probabilistic spatio-temporal tendencies of climate classes

in P2, respectively. Furthermore, occurrence probabilities of severe-arid (climate type in the region have tended to

increase and become rather conspicuous at most of the stations in P3 (15.8% in Birecik, 5.5% in Sanliurfa, 26.3%

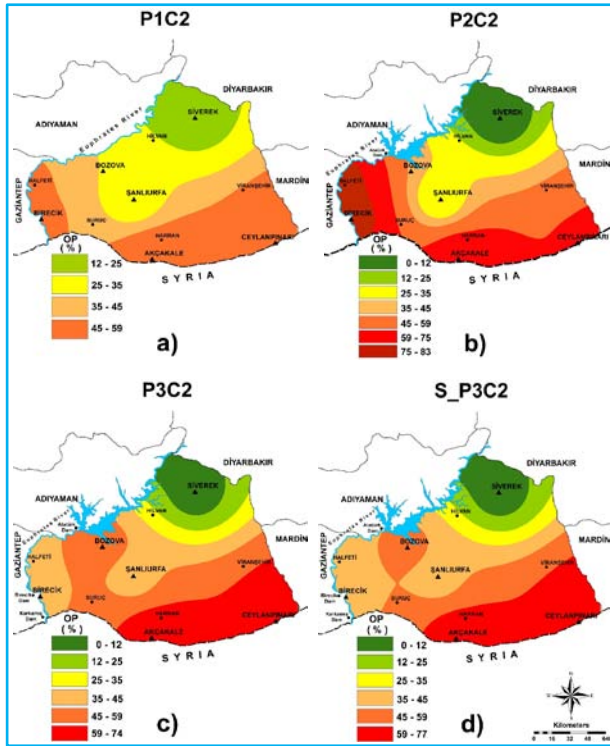
in Akcakale and Ceylanpinari). While occurrence probabilities of semi-arid (C3) climate type showed a decreasing tendency in the study area, arid (C2) climate class probabilities went up noteworthy (42.1% in Birecik, 52.6% in Bozova, 36.6% in Sanliurfa, 73.7% in Akcakale and Ceylanpinari) in P3. Interpretation of occurrence probabilities for the climate classes or types offered us to conclude that the nearer the stations are to the Syrian border, the higher the occurrence probabilities of arid (C2) climate type are over the study area.

The steady-state transitional probability matrix, viz., independent transition probability matrix, is obtained by raising the matrix to sufficiently high power, i.e., n -step, (Haan, 2002). In this study, steady-state probabilities of each station for P3 (2000-2018) was achieved by practicing the sequential multiplication rule in Haan (2002). Matrices reached a stable condition after one year (i.e., one-step) in Sanliurfa, four-year in Birecik and Akcakale, five-year in Siverek, Bozova and Ceylanpinari stations. Thus, the distant future for steady-state climatic conditions is not too far but about five-year over the study area. It was shown that stationary transition probabilities are independent of the initial state of the weather system over the area and removing the outliers from I_m series helped us to render the transition matrix of climate types to be regular. Steady-state probabilities of the climate classes were given in Table 6. According to the steady-state probabilities of each station for P3 in Table 6, severe-arid and arid-type climates are unlikely to be observed around Siverek station. This result may be attributed to the construction of a large dam, Atatürk Dam, by the station. However, over the long run, climate type is semi-arid 46.2% of the time, sub-humid 53.8% of the time around Siverek station located at the farthest point from the Syrian border and under the influence of the Atatürk Dam. Contrary to Siverek station, the probability of severe-arid climate type in any year in the distant future is 5.3%, 16.3%, 23.5% and 27.8% in Sanliurfa, Birecik, Ceylanpinari and Akcakale, respectively. Again, over the long run, climate type is expected to be arid 37%, 40%, 50%, 72% and 77% of the time in Sanliurfa, Birecik, Bozova, Akcakale and Ceylanpinari, respectively. Interpretation of results led us to conclude that the prevailing semi-arid climate types have been gradually vanishing in the study area and more severe weather conditions of severe-arid and arid climate types have been getting more and more obvious lately. Our research results support the postulate of IPCC (2014) and WMO (2019) because the small I_m , an indication of arid conditions, is directly related to an increase in temperature or a reduction in precipitation as well as humidity in the study area.

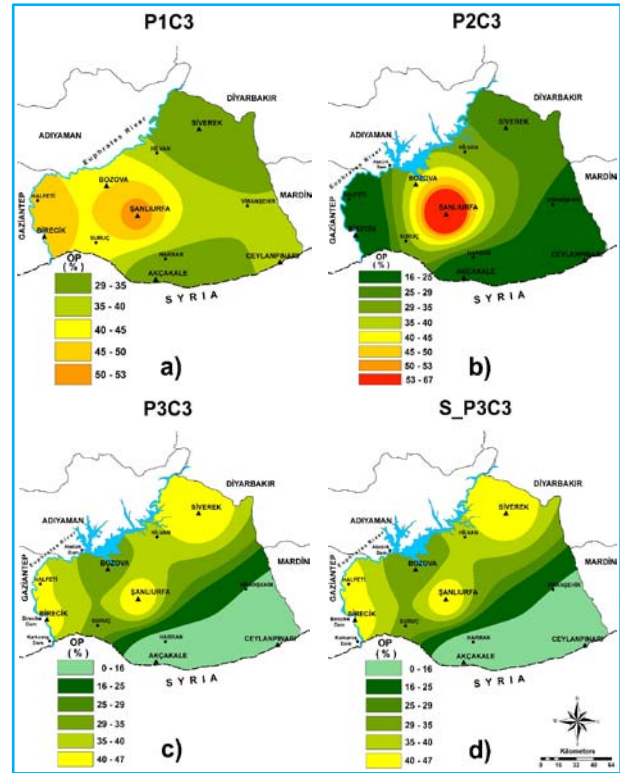


Figs. 4(a-d). Probabilistic spatiotemporal tendencies of severe-arid climate class (C1) for the three successive periods: P1: 1965-1981, P2: 1982-1999, P3: 2000-2018

Furthermore, the marginal probability vectors of stations for three successive periods (P1, P2, P3) and the steady-state probabilities (S_P3) for the third period are shown in Fig. 3. As seen clearly, the occurrence probabilities of C3 and C4 have tended to decrease by the periods. Contrarily, the probability of observing arid (C2) and severe-arid (C1) climate types have been liable to escalate substantially in the stations by decades. As seen in Fig. 3, steady-state probabilities support the retrograde climate types in favor of aridification in the study area. In this regard, it is unlikely that the humid climate class will be seen in Birecik in the distant future, but semi-arid and arid climates will act decisively. Nevertheless, Akcakale and Ceylanpinari stations have been much more prone to C1 (severe-arid) climate class. Water resources development projects materialized between 1981 and 2000, including the Atatürk Dam, have contributed to the development of a humid climate type at the nearby stations, i.e., Siverek, for a while. Probability results indicated clearly that it is unlikely to observe an arid climate class in Siverek in the distant future due to the effect of large-scale water resources development projects. Our findings regarding steady-state probabilities for climate classes are in accord with the results of Tonkaz



Figs. 5(a-d). Probabilistic spatiotemporal tendencies of arid climate class (C2) by successive periods



Figs. 6(a-d). Probabilistic spatiotemporal tendencies of semi-arid climate class (C3) for the three successive periods

and Cetin (2007) and Tonkaz *et al.* (2007). In summary, research findings suggested that the occurrence probability of severe-arid (C1) and Arid (C2) climate types in the region have tended to increase over time and become rather conspicuous over the study area. Furthermore, the semi-arid climate type (C3) has shown more stable behavior in the region. The occurrence probability of sub-humid climate class (C4) decreases from the first period to the third period. The study area has hardly ever experienced humid (C5) and very humid (C6) climate types and there has been a very slim chance to occur in the future.

3.5. Probabilistic spatiotemporal tendencies of climate classes

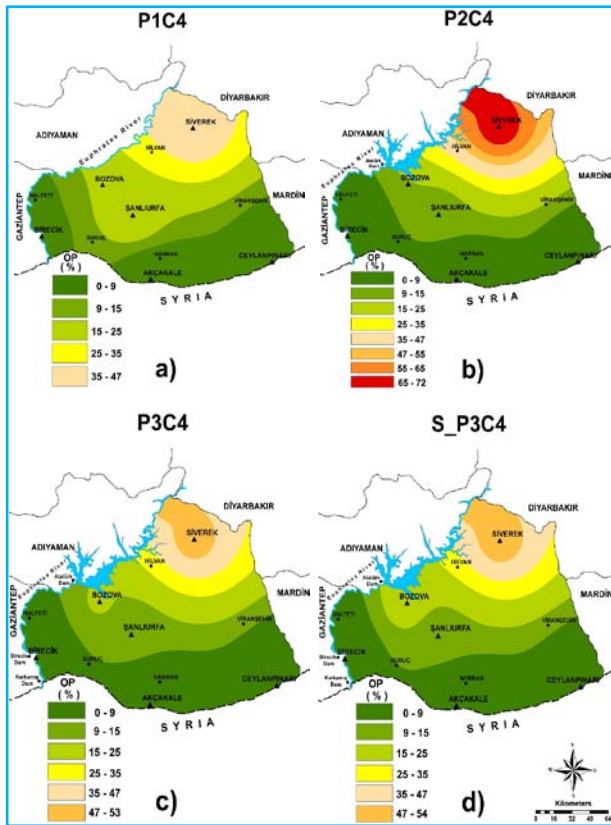
Spatiotemporal tendencies of severe-arid climate class (C1) : Maps of probabilities given in Table 6 were generated with a cell size 100 m by 100 m over the study. The procedure implemented in C1 map generation was repeated to map probabilities of C2, C3 and C4. Probability maps for severe-arid climate type by period were given in Fig. 4.

As seen in Figs. 4(a-d), areal coverage of the probability of occurrence of severe-arid climate class (C1)

has gradually spread out by the periods. More importantly, occurrence probabilities are higher in the southern parts of the study area and its areal expansion shows steadily continuous increasing behavior from the south to the north. Although the Atatürk, Karkamış and Birecik Dams were gradually operationalized in 1992, 1999 and 2000, respectively, C1 climate class had inconceivably continued spreading out from Halfeti, Birecik, Suruc, Harran, Akcakale, Ceylanpinari and Viranşehir corridor to the Atatürk Dam (Fig. 4). As seen in Figs. 4 (c & d), the difference between the spatial distribution of marginal probability values (P3C1) and steady-state transitional probabilities (S_P3C1) is unlikely differentiable due to the fact that C1 type climate which is undesirable has become dominant at most of the stations as period 3 approaches the end.

Spatiotemporal tendencies of arid climate class(C2) : Occurrence probabilities (OP) of the C2 climate class have gradually increased from south to north by periods. As seen in Figs. 5(a-c), the probability of arid climate type is comparatively small and the areal extent of probabilities greater than 60% is limited to P1.

However, in P2, both the magnitude and areal extent of marginal probabilities have unusually increased in the



Figs. 7(a-d). Probabilistic spatiotemporal tendencies of sub-humid climate class (C4) for the three successive periods

area. After the construction of the Atatürk Dam, the occurrence probability of the C2 climate class varied from 59% to 83% in period 3. In the first period, the occurrence probability of the C2 climate type varied between 35% to 59% in the region. In the 3rd period, the occurrence probability of the C2 climate class decreased from 75%-83% to 35%-45% in the environs of Birecik and Halfeti. This change may be attributed to the construction of Birecik and Karkamış Dams constructed in the context of the GAP. Nonetheless, the C2 climate class has continued spreading out northward as seen in the steady-state transitional probabilities [S_{P3C2} in Fig. 5(d)], irrespective of large-scale water reservoirs.

Spatiotemporal tendencies of semi-arid climate class (C3) : As seen in Figs. 6(a&b), the probability of C3 (semi-arid) climate class is more than 40% around Sanliurfa, Bozova, Suruc, Halfeti and Birecik in the P1.

In due course of time, high occurrence probabilities of C3 showed a gradual decreasing tendency from Halfeti and Birecik towards Sanliurfa station in P2. This tendency might be attributed to the construction of large dams

around Halfeti and Birecik in P2 because Sanliurfa, which is under the influence of desert climate caused by air currents from Syria, is located at the center of the study area and far from the Euphrates river bed. At the end of the P2, the construction of the Atatürk Dam was fully completed. The occurrence probability of the C3 climate class in P3 showed a gradual decrease from north to south and the occurrence probability of the C3 climate type was less than 16% around Akcakale, Ceylanpinari and Viransehir, where arid and severe-arid climate types have already substituted in a gradual way for semi-arid climate type in P3. Considering all periods and stable (steady-state) transition probabilities S_{P3C3} given in Fig. 6(d), it may be concluded that the areas of the C3 climate type have already shifted to either C2 (arid) or C1 (severe-arid) climate class.

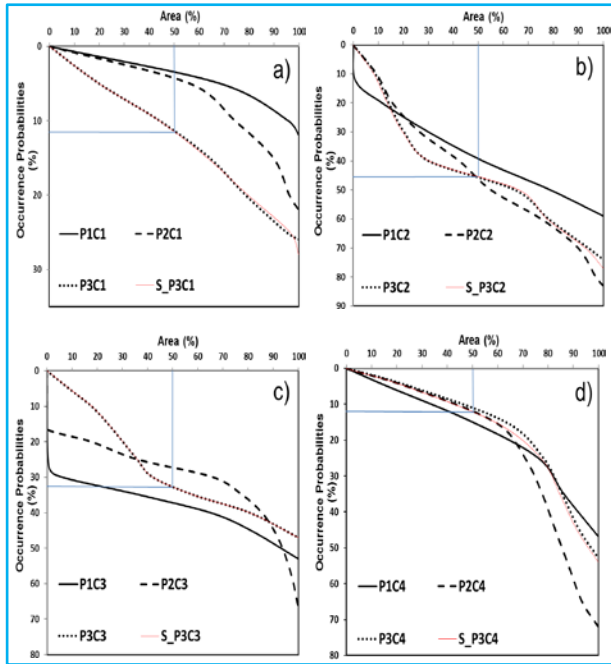
Spatiotemporal tendencies of sub-humid climate class (C4) : As seen in Fig. 7(a), the probability of observing C4 around Siverek and Hilvan districts was between 25% and 47% in P1.

However, after the Atatürk Dam was constructed, the probability of C4 varied from 25% to 72% and areal coverage increased substantially in P2. On the other hand, during period 3, the influence of large reservoirs on C4 climate type started to vanish and levelled off, indicating stable conditions as seen in Figs. 7(c&d). It is important to emphasize that the probability of sub-humid climate type (C4) in a year in the distant future is less than 15% in 65% of the study area. Thus, over the long run, as seen in Fig. 7(d), only 15% of the study area will experience sub-humid climate type with a probability of 35% to 54%.

In summary, the areal extent of severe-arid (C1) and arid (C2) climatic classes have consistently continued to spread from the south to the north. The semi-arid climate type (C3) has shown more or less stable behavior in the region and has tended to shift towards the arid climate type (C2) in the future. The occurrence probability of sub-humid climate class (C4) decreases from the first period to the third period, expanding areally from the south to the north. Meanwhile, the study area has hardly ever experienced a humid (C5) climate type and it is unlikely that a very humid (C6) climate type to occur in the future.

3.6. Practical implications of hypsometric curves for occurrence probabilities

Climate class maps may be a useful tool to expose the spatial distribution of occurrence probabilities, *i.e.*, marginal or fixed probabilities, of climate types. However, since any climate type prevails over an area (USEPA, 2021), it is important to designate areal coverage (Speight, 2019) affected by a particular climate type as shown in



Figs. 8(a-d). The areal coverage of occurrence probabilities of climate classes for the three successive periods

Keskiner *et al.* (2020). By practicing this approach, hypsometric curves for the three distinct periods considered were derived from occurrence probabilities as seen in the Fig. 8.

Reports by IPCC (2013 and 2014) highlighted that Mediterranean countries, including Turkey, will be affected irreversibly by the climate change phenomenon. The study area is particularly critical for the prevailing climate types. In this context, the “severe-arid” (C1) climate class has continued inconceivably to spread. This increase is evident in the hypsometric curve [Fig. 8(a)]. During periods P1 and P2, the occurrence probability of C1 was less than 4% in 50% of the study area. Surprisingly, the occurrence probability of C1 reached 12% in 50% of the area at the end of P3 and under stable conditions; and occurrence probability varied from 12% to 26% over the remaining half of the area, indicating severe-arid zone encroachment from south to north.

Hypsometric curves in Fig. 8(b) show a decreasing trend in occurrence probabilities of “arid” climate class (C2) over the area in the first period. However, a myriad of large dams was put into operation in P2. Therefore, this practice developed uncertainty in climate types preponderant over the area and in turn, the C2 climate class hypsometric curves intersected each other by making oscillations. It was concluded that these curves show similar behavior and this climate class is likely to

represent the south of Sanliurfa province as the dominant climate class in the future. Finally, the occurrence probability of arid climate (C2) in P3 as well as under steady-state conditions ranged between 46% and 77% in half of the area.

As seen in Fig. 8(c), occurrence probabilities of semi-arid climate class (C3) were between 30% and 51% in P1, showing that the dominant climate type was C3 over the study area in the 1960s and before. While the occurrence probability of C3 in P1 is higher than in the other two periods, the occurrence probability of C3 has decreased remarkably (less than 35% in 75% of the area) at the end of P2. This is a good indication that the climate type over the area has already reached stable conditions at the end of P3. The decrease in occurrence probabilities in P2 could be attributed to dams constructed in the context of water resources development projects.

Given the climatic and geographic features of the study area, a sub-humid climate type (C4) should be observed in any station, except for Siverek. Fig. 8 justifies our postulation. The occurrence probability of C4 was less than 23% in 70% of the area in P1 and P2. Under steady-state conditions, the probability of being in C4 is only 20%.

4. Conclusions

Climate types are subject to evolve due to global warming and inherited uncertainties in climate, leading to a shift in drought-prone areas in fragile landscapes. Therefore, by considering time, characterization of the climate types and determination of spatiotemporal trends in climate types are of great importance in large-scale development project areas like the Southeastern Anatolia Project (GAP in Turkish) area, including 13 irrigation and hydropower schemes and the construction of 22 dams and 19 hydroelectric power plants on both the Tigris and the Euphrates rivers, in Turkey. This research was conducted in Sanliurfa province, located in GAP area, with an arid to semi-arid climate. Erinc’s Drought/Aridity Index (*ImorEDI*) was adopted to quantify climate types for three consecutive periods. Based on the research results, the following conclusions could be drawn:

- (i) Physical region-wide developments and starting and finalizing dates of the hydraulic works in river basins should be considered in drought characterisation studies. Therefore, dividing the data into periods helped us derive more concise and logical conclusions on how the climate has evolved over time.
- (ii) The severe-arid (C1) and arid (C2) climate types, which were not spatially dominant over the study area in

the 1960s and 1970s, have already started to expand spatially from south to north and showed spatiotemporal increasing tendencies in the region.

(iii) The semi-arid climate type (C3) has shown more stable behavior in the region. But, the semi-arid (C3) climate type showed a shifting behavior towards the arid climate type (C2) in the future.

(iv) The sub-humid climate class (C4) decreases from the first period to the third period, expanding areally from the south to the north and will be expected to be dominant in a very small area located in the north of the Atatürk Dam in the future.

(v) Construction of large hydraulic structures, *i.e.*, reservoirs and opening large areas to irrigation has had no positive effect on the persistency of the dominant semi-arid climate regime. The transition from a semi-arid to an arid regime has progressively continued as time varies.

(vi) Markov modelling results suggested that the study area has hardly ever experienced humid (C5) and very humid (C6) climate types and there has been a very slim chance to occur in the future. Additionally, it is unlikely that Atatürk, Birecik and Karkamis Dams will prevent the occurrence of spatio-temporal aridity from south to north in Sanliurfa.

(vii) In order to mitigate the negative effects of climate change and arid zone encroachment onto irrigation schemes, we suggested forestation and forest management practices be planned and implemented urgently in the environs of Sanliurfa.

(viii) Spatial enumeration of climate types and steady-state occurrence probabilities by Markov chain modelling might be a remedy for deriving concrete information on the fragile environment of large-scale integrated water resources development project areas like the GAP area in Turkey. That is why it was strongly recommended that spatio-temporal climate change studies be periodically conducted in the whole of the GAP area.

Disclaimer: The contents and views expressed in this study are the views of the authors and do not necessarily reflect the views of the organizations they belong to.

References

- Ajaykumar, B. N. and Gopinath, G., 2018, "Geospatial techniques for the analysis of hypsometric parameters of a humid tropical river basin, south western Ghats, India", *Carpathian Journal of Earth and Environmental Sciences*, **13**, 2, 465-476.
- Aydın, S. Simsek, M. Cetinkaya, G. and Oztürk, M. Z., 2019, "Regime Characteristics of Turkey's Climatic Regions Determined Using TheErinc Precipitation Efficiency Index", In: Proceedings of 1st Istanbul International Geography Congress, June 20-22, 752-760.
- Caglak, S. Ozlu, T. and Gunduz, S., 2016, "The Analysis of climatic characteristics of Sanliurfa with interpolation techniques", *The Journal of International Social Research*, **9**, 45, 360-372.
- Cetin, M. and Diker, K., 2003, "Assessing drainage problem areas by GIS: A Case study in the eastern Mediterranean region of Turkey", *Irrigation and Drainage*, **52**, 343-353.
- Cetin, M., 2020, "Agricultural Water Use. In: Harmancioglu, N., Altinbilek, D. (Eds.), *Water Resources of Turkey: World Water Resources*", Vol. 2, Springer, Cham, 257-302.
- Erinç, S., 1965, "YağışMüessiriyetiÜzerine Bir Denemeve Yeni Bir İndis", Istanbul University Institute Release, Baha Press (in Turkish).
- ESRI (Environmental Systems Research Institute), 2021, "Implementing Inverse Distance Weighted", [http://webhelp.esri.com/arcgisdesktop/9.2/index.cfm?TopicName=Implementing_Invers_e_Distance_Weighted_\(IDW\)](http://webhelp.esri.com/arcgisdesktop/9.2/index.cfm?TopicName=Implementing_Invers_e_Distance_Weighted_(IDW)) (accessed 25 July, 2021).
- Feddema, J. J., 2005, "A revised Thornthwaite-Type global climate classification", *Physical Geography*, **26**, 6, 442-446.
- FFDIA (Federation of Food & Drink Industry Associations of Turkey), 2017, "Climate change and sustainable agriculture in Turkey", <https://www.tgdf.org.tr/wp-content/uploads/2017/10/iklim-degisikligi-rapor-elma.compressed.pdf> (accessed 25 July, 2021).
- Fidan, I., 2011, "Drought Analysis by Standardized Precipitation Index (SPI) and Determination of Drought Occurrence Probabilities Through Using Markov Chains in The Eastern Mediterranean Region", MSc, Cukurova University, Adana, Turkey.
- GDM (General Directorate of Mapping), 2021, "Surface area of Turkey's provinces and districts", <https://www.harita.gov.tr/urun/il-ve-ilce-yuzolcumleri/176> (accessed 25 July, 2021).
- Grinstead, C. M. and Snell, J. L., 2012, "Introduction to Probability. Second Revised Edition", *Providence : American Mathematical Society*, 405-470.
- Grubbs, F. E., 1969, "Procedures for detecting outlying observations in samples", *Technometrics*, **11**, 1, 1-21.
- Haan, C. T., 2002, "Statistical Methods in Hydrology", Second Edition, The Iowa State University Press, Ames, IO.
- Habibi, B. Meddi, M. Torfs, P. J. J. F. Remaoun, M. and Van Lanen, H. A. J., 2018, "Characterisation and prediction of meteorological drought using stochastic models in the semi-arid Chélliff-Zahrez Basin (Algeria)", *Journal of Hydrology, Regional Studies* **16**, 15-31.
- Han, F. Zhang, Q. Buyantuev, A. Niu, J. Liu, P. Li, X. Kang, S. Zhang, J. Chang, C. and Li, Y., 2015, "Effects of climate change on phenology and primary productivity in the desert steppe of inner Mongolia", *Journal of Arid Land*, **7**, 2, 251-263.
- Houghton, D. D., 2002, "Introduction to Climate Change: Lecture Notes for Meteorologists", Secretariat of The World Meteorological Organization, Geneva-Switzerland, WMO-No.926.
- Inceyol, Y. and Cay, T., 2017, "The effects of delays in irrigation implementation projects and irrigation system changes on land consolidation works performed in Harran Plain", *Journal of Engineering Science of Adiyaman University*, **7**, 54-62.

- IPCC (Intergovernmental Panel on Climate Change), 2013, "The intergovernmental panel on climate change, summary for policymakers. In: Climate change 2013: The physical science basis. Contribution of working group I to the fifth assessment report of the intergovernmental panel on climate change", Stocker, T. F., Qin, D., Plattner, G. K., Tignor, M., Allen, S. K., Boschung, J., Nauels, A., Xia, Y., Bex, V., Midgley, P. M. (Eds.), Cambridge University Press, Cambridge, United Kingdom and New York, NY, USA, 1-29.
- IPCC (Intergovernmental Panel on Climate Change), 2014, "The intergovernmental panel on climate change. Climate change 2014 synthesis report summary for policymakers", https://www.ipcc.ch/site/assets/uploads/2018/02/AR5_SYR_FINAL_SPM.pdf (accessed 25 July, 2021).
- Iyigun, C. Turkeş, M. Batmaz, I. Yozgatligil, C. Purutcuoğlu, V. Koc, E. K. and Öztürk, M. Z., 2013, "Clustering current climate regions of Turkey by using a multivariate statistical method", *Theoretical and Applied Climatology*, **114**, 95-106.
- Karamouz, M. Szidarovszky, F. and Zahraie, B., 2003, "Water Resources Systems Analysis with Emphasis on Conflict Resolution", ISBN: 1- 56670-642-4, CRC Press LLC, USA.
- Kesici, T. and Kocabaş, Z., 1998, "Biostatistics", Ankara University Faculty of Pharmacy, Ankara, 235-239.
- Keskiner, A. D. Cetin, M. and Nagano, T., 2019, "Mapping spatio-temporal tendencies of climate types in geographic information systems (GIS) media: A Case study in Sanliurfa and its environs", *Mustafa Kemal University Journal of Agricultural Sciences*, **24**, 232-240.
- Keskiner, A. D. Cetin, M. Şimsek, M. and Akin, S., 2020, "Design of small earthen dam reservoirs lying in drought-prone areas: An application to the Seyhan River Basin", *İMO Teknik Dergi*, **31**, 5, 10189-10210.
- Komuscu, A. U. Erkan, A. and Oz, S., 1998, "Possible impacts of climate change on soil moisture availability in the Southeast Anatolia Development Project Region (GAP): An analysis from an agricultural drought perspective", *Climatic Change*, **40**, 519-545.
- Kumar, A. Tripathi, P. Singh, K. K. and Mishra, A. N., 2011, "Impact of climate change on agriculture in eastern Uttar Pradesh and Bihar states (India)", *MAUSAM*, **62**, 2, 171-178.
- Landau, S. and Everitt, S. B., 2004, "A Handbook of Statistical Analyses", A CRC press company, Washington.
- Li, Y. Yao, N. Sahin, S. and Appels, W.M., 2017, "Spatiotemporal variability of four precipitation-based drought indices in Xinjiang, China", *Theoretical and Applied Climatology*, **129**, 1017-1034.
- Loucks, D. P. and van Beek, E., 2005, "Water Resources Systems Planning and Management: An Introduction to Methods, Models and Applications. Studies and Reports in Hydrology", UNESCO Publishing, Italy.
- Mieruch, S. Noel, S. Bovensmann, H. Burrows, J. P. and Freund, J. A., 2010, "Markov chain analysis of regional climates", *Nonlinear Processes in Geophysics*, **17**, 651-661.
- NASA (National Aeronautics and Space Administration), 2021a, "Overview: Weather, global warming and climate change", <https://climate.nasa.gov/resources/global-warming-vs-climate-change/> (accessed 25 July, 2021).
- NASA (National Aeronautics and Space Administration), 2021b, "The causes of climate change", <https://climate.nasa.gov/causes/> (accessed 25 July, 2021).
- NRC (National Research Council), 2002, *Abrupt Climate Change: Inevitable Surprises*, Washington, DC., The National Academies Press.
- Panwar, P. Bhatt, V. K. Pal, S. Loria, N. Alam, N. M. Sharma, N. K. and Mishra, P. K., 2020, "Vulnerability of agricultural households to climate change in hill state of north Western Himalaya", *MAUSAM*, **71**, 2, 199-208.
- Reis, M. and Dotal, H., 2016, "Determining hydrological drought probability in future using Markov Chain model for Kahramanmaraş City", *Journal of Forestry Faculty*, **16**, 1, 34-43.
- Ryan, B. F. Joiner, B. L. and Cryer, J. D., 2012, "Minitab Handbook: Updated for release 16, Sixth Edition", Brooks/Cole Publishing Co., Boston.
- Savo, V. Lepofsky, D. Benner, J. P. Kohfeld, K. E. Bailey, J. and Lertzman, K., 2016, "Observations of climate change among subsistence-oriented communities around the world", *Nature Climate Change*, **6**, 462-474.
- Shevnina, E. and Silaev, A., 2019, "The probabilistic Hydrological MARCS^{HYDRO} (the MARKov Chain System) Model: Its structure and Core Version 0.2", *Geoscientific Model Development*, **12**, 2767-2780.
- Singh, N. Mall, R. K. Sonkar, G. Singh, K. K. and Gupta, A., 2018, "Evaluation of RegCM4 climate model for assessment of climate change impact on crop production", *MAUSAM*, **69**, 3, 387-398.
- Speight, J. G., 2019, *Global Climate Change Demystified*, Hoboken, NJ: Wiley.
- Stedinger, J. R., 2017, "Flood Frequency Analysis Chapter 45. In: Singh VP (ed) *Handbook of Applied Hydrology*", McGraw-Hill Education, New York, 76-1-76-8.
- Taha, H. A., 2007, "Operations Research: An Introduction", Pearson Prentice Hall, New Jersey.
- Tonkaz, T. and Cetin, M., 2007, "Effects of urbanization and land-use type on monthly extreme temperatures in a developing semi-arid region, Turkey", *Journal of Arid Environments*, **68**, 143-158.
- Tonkaz, T. Cetin, M. and Tülüciü, K., 2007, "The Impact of water resources development projects on water vapor pressure trends in a semi-arid region, Turkey", *Climatic Change*, **82**, 195-209.
- Towler, E. Rajagopalan, B. Gilleland, E. Summers, R.S. Yates, D. and Katz, R. W., 2010, "Modeling hydrologic and water quality extremes in a changing climate: A statistical approach based on extreme value theory", *Water Resources Research*, **46**, 11, W11504.
- TSMS (Turkish State Meteorological Service), 2021, "Climate classification", <https://www.mgm.gov.tr/iklim/iklim-siniflandirmalari.aspx> (accessed 25 July, 2021).
- Turan, E. S., 2018, "Turkey's drought status associated with climate change", *Journal of Natural Hazards and Environment*, **4**, 1, 63-9.
- UNDP (United Nations Development Programme), 2021, "Turkey's second national communication-in progress",

<https://www.adaptation-undp.org/projects/turkeys-second-national-communication-progress>, (accessed 25 July, 2021).

USEPA (United States Environmental Protection Agency), 2021, "Climate change indicators: Weather and climate", <https://www.epa.gov/climate-indicators/weather-climate> (accessed 25 July, 2021).

Vivoni, E. R. Benedetto, F. D. Grimaldi, S. and Eltahir, E. A. B., 2008, "Hypsometric control on surface and subsurface runoff", *Water Resources Research*, **44**, W12502.

WMO (World Meteorological Organization), 2019, "WMO statement on the state of the global climate in 2018", WMO-No.1233, https://library.wmo.int/doc_num.php?explnum_id=5789 (accessed 25 July, 2021).

Highlights

1. Arid areas are prone to expand spatially from the south to the north in the southeastern Anatolia region (in the GAP area) of Turkey.
2. Aridity shows spatio temporal increasing tendencies in the region.
3. Dividing Erinc's aridity/drought index series into three periods (P1, P2 and P3), non-overlapping and successive, helped us to determine the likely trend in climate types classes.
4. The development of large-scale water resources projects by constructing large dams such as the Atatürk Dam and opening large areas for irrigation in the GAP region could not prevent humid climate types from fading away.

